hkl_phase, the bias is reduced to about 1% and does not show systematic deviations.

It should be noted, however, that the phase constants developed using such a calibration approach will only be applicable to the sample suite and preparation conditions for which it was developed. The calibration process will need to be repeated if there are significant changes to the sample suite or sample-preparation conditions.

3.9.10.3.4. *Whole-pattern-refinement effects*

One of the distinct advantages of structure-based whole-pattern fitting for QPA is that no standards need to be prepared because the structure for each phase provides the phase constant *ZMV*; the unit-cell dimensions allow the calculation of the cell volume *V* and the unit-cell contents provide the mass *ZM* (Bish & Howard, 1988; Hill & Howard, 1987). These values are used, along with the Rietveld scale factor *S*, in equation (3.9.26) to derive the phase abundance. This is especially useful for complex systems where the preparation of multiple standards would add considerably to the analytical complexity.

An additional advantage is the ability to refine the crystal structure (unit-cell dimensions and site-occupation factors, for example), when the data are of sufficiently high quality, in order to obtain the best fit between observed and calculated patterns. In addition to updating the *ZMV* value, the site occupancies are contained in the structure-factor calculation and, therefore, will change the relative reflection intensities and have an impact on the scale factor and QPA. Other structural parameters that have a strong effect on the scale factor and QPA are the atomic displacement parameters (ADPs). Strong correlation between the ADPs and amorphous material concentration has been shown by Gualtieri (2000) and Madsen *et al.* (2011).

This leads to the question: which crystal structure should be selected for QPA? Databases contain multiple entries for the same phase with the structures determined using different methods. While ADPs and site-occupation factors determined using neutron diffraction and single-crystal analysis should be favoured over those determined using X-ray powder data, many database entries do not have refined ADPs for all (and in some cases, any) atoms. Often, arbitrarily chosen default values of 0.5 or 1.0 Å^2 for B_{eq} are entered for all atoms, but this should be viewed or used with great caution. There is clearly a need to carefully evaluate the crystal-structure data used for QPA. This is particularly worth mentioning in view of the advent of new 'user-friendly' software that automatically assigns crystal structures after having performed the phase identification.

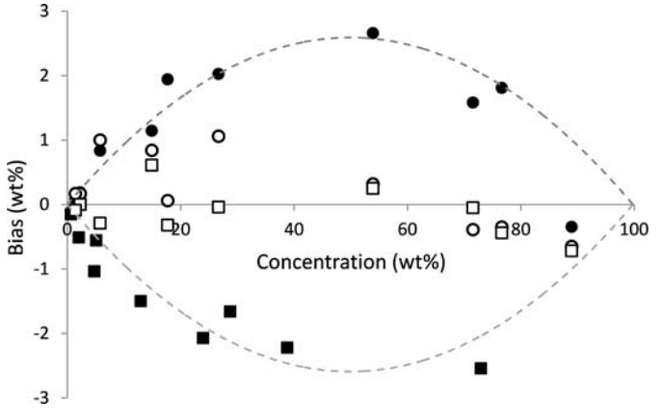

Figure 3.9.20
Bias as a function of phase concentration for industrial salt samples for (i) structure-based QPA (filled symbols) and (ii) calibrated hkl_phase (open symbols) for halite (circles) and sylvite (squares). The broken lines indicate the trend of the bias for structure-based QPA. Data are courtesy of K+S AG, Germany.

Empirical profile-shape models contribute significantly to the complexity (and correlations) of whole-powder-pattern fitting for QPA because of the large number of phases and multiple parameters required to model the profile shape of each phase. The use of convolution-based profile fitting [in, for example, *BGMN* (Bergmann *et al.*, 1998, 2000) and *TOPAS* (Bruker AXS, 2013)] greatly reduces the number of parameters, because the instrument-resolution function (which is constant for a given setup) can be separated from sample-related peak broadening. The instrument component can be refined using a standard and then fixed for subsequent analysis. The sample contribution to peak width and shape can then be related directly to crystallite size and microstrain using a minimal number of parameters. The reduction of the total number of parameters reduces the refinement complexity and the chance of parameter correlation.

The choice of the function used to model the pattern background may also have a strong influence on amorphous content (Gualtieri, 2000; Madsen *et al.*, 2011). Given that the intensities of both the background and the amorphous contribution vary slowly as a function of 2θ, it is inevitable that there will be a high degree of correlation between them. Hence, any errors in determining the true background will result in errors in amorphous phase determination. A simple approach is to use a background function with a minimal number of parameters. A more exact approach requires the separation of the amorphous contribution from background components such as Compton scattering and parasitic scattering by the sample environment and air in the beam path. This is routinely done in pair distribution function (PDF) analysis; details can be found in Chapter 5.7 in this volume and in Egami & Billinge (2003).

Another parameter that correlates with the pattern background is the width of broad peaks for phases of low concentration. If allowed to refine to very large width values, the peaks are 'smeared' over a broad range of the pattern with no clear distinction between peaks and background. The same issue applies when there is a high degree of peak overlap, particularly at high angles, leading to severe under- or over-estimation of the phase. The careful use of limits for either crystallite size or corresponding parameters in empirical peak-shape modelling assists in minimizing this effect.

There can be a subtle interplay between the profile-shape function and the pattern background that has an impact on whole-pattern fitting (Hill, 1992). The data in Fig. 3.9.21, collected using a Cu tube and an Ni $K\beta$ filter, exhibit low-angle truncation of the peak tails at the β-filter absorption edge. On the high-angle side, the anatase peak displays a wide tail which extends to the position of the strongest rutile peak at about 27.5° 2θ. In this case, rutile is present as a minor phase and the error in the background determination using conventional peak-profile modelling (Fig. 3.9.21*a*) introduces about 0.5% bias in the rutile QPA. The use of a more accurate profile model that incorporates the effect of the β-filter absorption edge (Fig. 3.9.21*b*) serves to improve the accuracy (Bruker AXS, 2013).

3.9.10.3.5. *Element analytical standards*

XRD-based derivation of elemental abundances relies on (i) the QPA abundances, and (ii) the assumed or measured stoichiometry of the crystalline phases. The accuracy of the QPA

Table 3.9.6
Compositional analysis of the Dillinger Hütte iron-ore certified reference material SX 11-14, (i) derived from QPA results, taking into account the nominal stoichiometry of the phases (XRD) and (ii) the certified analyses (Cert) (Knorr & Bornefeld, 2013)

Phase	wt%		Fe	FeO	SiO_2	Al_2O_3	MgO	CaO	K_2O	Na_2O	C
Haematite	0.37		0.26	—	—	—	—	—	—	—	—
Goethite	3.86		2.43	—	—	—	—	—	—	—	—
Magnetite	85.97		62.21	26.68	—	—	—	—	—	—	—
Quartz	5.73		—	—	5.73	—	—	—	—	—	—
Gibbsite	0.71		—	—	—	0.46	—	—	—	—	—
Talc	1.79		—	—	1.13	—	0.57	—	—	—	—
Orthoclase	0.30		—	—	0.19	0.05	—	—	0.05	—	—
Albite	0.89		—	—	0.60	0.18	—	—	—	0.10	—
Calcite	0.40		—	—	—	—	—	0.22	—	—	0.19
			Fe	FeO	SiO_2	Al_2O_3	MgO	CaO	K_2O	Na_2O	C
		XRD	64.89	26.68	7.66	0.70	0.57	0.22	0.05	0.10	0.19
		Cert	65.55	27.20	7.47	0.27	0.56	0.42	0.06	0.08	0.12
		Bias	−0.66	−0.52	0.19	0.43	0.01	−0.20	−0.01	0.02	0.07

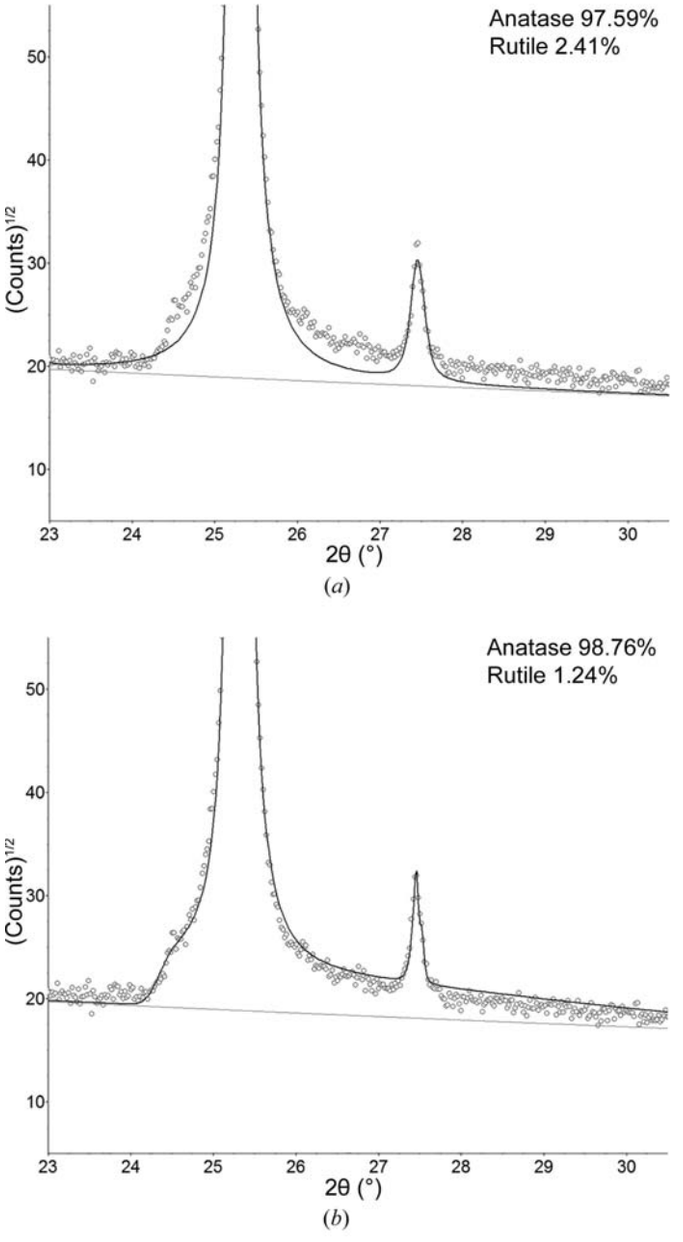

Figure 3.9.21
Profile fit of anatase and rutile (*a*) without and (*b*) with a $K\beta$ filter absorption-edge correction.

result may then be evaluated by comparing the calculated elemental abundances with those determined by traditional chemical-analysis techniques. However, for the best level of agreement, this method requires that the composition of the crystalline phases be well defined. A complication, in particular for minerals, is that idealized compositions may be reported but do not necessarily match the actual composition of the species present in the sample. Where possible, detailed phase analysis using microbeam techniques should be undertaken to establish the true composition for each phase. A complication that serves to decrease the agreement is that chemically based compositional analysis does not distinguish between crystalline and amorphous phase content, while the diffraction-based QPA usually measures only the crystalline phases. Generally, the composition of amorphous phases may not be known accurately and even highly crystalline material can contain amorphous components because of non-diffracting surface layers of the grains (Cline *et al.*, 2011).

An example demonstrating the level of agreement that can be achieved is that of the iron-ore certified reference material SX 11-14 from Dillinger Hütte (Fig. 3.9.22). The material is moderately complex and consists of nine distinct mineral species. The data were measured with Co $K\alpha$ radiation and analysed using Rietveld-based QPA in *TOPAS* (Bruker AXS, 2013). The phase abundances are converted to elemental and oxide compositions for comparison with the certified elemental analyses (Table 3.9.6). There is excellent agreement between the XRD results and the chemical analysis with bias values better than ±1 wt%.

3.9.10.3.6. *Phase-specific methods: diffraction SRMs, round-robin samples and synthetic mixtures*

In contrast to elemental compositional analysis, where standard reference materials (SRMs) are widespread, there are only a very limited number of SRMs available for diffraction-based QPA. Prominent examples are SRMs for the cement industry [NIST reference material clinker 8486 (Stutzman & Leigh, 2000) and ordinary Portland cement NIST SRM 2686] or ceramics materials (silicon nitride CRM BAM-S001) (Peplinski *et al.*, 2004). Similar to elemental standards, the certified values do not necessarily represent the true composition. Rather, they are published values that are typically averaged over the results from different independent methods, instruments and laboratories. Therefore, confidence limits of concentrations are provided that may be much larger than estimated standard deviations of concentrations within a single laboratory.